The Crystal Structure of Paratacamite, $Cu_2(OH)_3Cl$

By M. E. Fleet

Department of Geology, University of Western Ontario, London, Ontario, Canada

Paratacamite, $Cu_2(OH)_3Cl$, is rhombohedral with $a = 13.654$ (5) Å, $c = 14.041$ (6) Å, space group $R\bar{3}$ (C_{3i}^2), $Z = 24$. It has a well developed substructure with $a' = a/2$, $c' = c$, apparent space group $R\bar{3}m$. The crystal structure has been determined by trial-and-error, after confirmation that the substructure has the rhombohedral $Co_2(OH)_3Cl$ crystal structure, and refined to a weighted residual index of 0·036 using 1027 reflexions collected on a single-crystal diffractometer with Mo $K\alpha$ ($\lambda = 0.7107$ Å) radiation. Although three quarters of the Cu atoms are coordinated to four near O atoms and two distant Cl atoms, giving the expected (4 + 2) configuration, three sixteenths of the Cu atoms have (2 + 4) configurations, with two O atoms at 1·93 Å and four O atoms at 2·19 to 2·20 Å, and one sixteenth of the Cu atoms have six equivalent O atoms at 2·12 Å. The positions of the H atoms suggest O–H$\cdots$Cl associations, three hydrogen bonds being directed to each Cl. Analogous hydrogen-bonding schemes are predicted for the other two $Cu_2(OH)_3Cl$ polymorphs, atacamite and botallackite. The O–Cu–O and O–Cu–Cl bond angles associated with shared coordination edges are all significantly less than 90° suggesting that the filled t_{2g} orbitals on the Cu atoms do not screen the atomic charges very effectively in these directions.

Introduction

$Cu_2(OH)_3Cl$ occurs in a variety of polymorphic forms, atacamite (orthorhombic), paratacamite (rhombohedral) and botallackite (monoclinic). The crystallographic properties of these and of related metal hydroxyhalides have been summarized by Oswald & Feitknecht (1964). Paratacamite and atacamite are common secondary minerals in areas of copper mineralization and frequently form as corrosion products of Cu-bearing metals. The relative stabilities of the two minerals are unknown although atacamite may be more stable at room temperature (Oswald & Feitknecht, 1964) and paratacamite formation is favoured in solutions of relatively low $CuCl_2$ concentration (Sharkey & Lewin, 1971).

Paratacamite was originally described by Smith (1906) in material from the Herminia and Generosa mines at Sierra Gorda, Chile, and was re-established as a mineral, distinct from atacamite, by Frondel (1950). As a result of a single-crystal Weissenberg study, Frondel reported that the symmetry of paratacamite is rhombohedral with the hexagonal unit-cell parameters $a = 13.68$ and $c = 13.98$ Å, $Z = 24$. There is a very pronounced pseudo-cell (subcell) with $a' = a/2$ and the true structure can be considered as a superstructure developed by an ordered arrangement of the substructure.

On the basis of similarity of unit cells, de Wolff (1953) proposed that the substructure of paratacamite has the $Co_2(OH)_3Cl$ structure shown by de Wolff to be in space group $R\bar{3}m$ with one quarter of the Co atoms, in Co(1) positions, coordinated to six equivalent O atoms and the remaining Co atoms, in Co(2) positions, coordinated to four O atoms and two Cl. Oswald & Feitknecht

substantiated this structural assignment through comparison of X-ray powder diffraction patterns of the two phases. In the atacamite structure (Brasseur & Toussaint, 1942; Wells, 1949) the Cu atoms are in stretched octahedral coordination. All of the Cu atoms have four nearest O atom neighbours, but one half of the Cu atoms, in Cu(1) positions, have two distant Cl atom neighbours, completing their coordination octahedra, and the remaining Cu, in Cu(2) positions, have one distant Cl and one distant O atom neighbours. The Cu atoms in botallackite are coordinated in similar ways (Voronova & Vainshtein, 1958). The stretching of Cu^{2+} coordination octahedra, giving (4 + 2) configurations, is usually attributed to Jahn–Teller distortion, arising through unequal $3d$ electron population of the e_g orbitals on the Cu^{2+} atoms. Since the Cu(1) position in the $Co_2(OH)_3Cl$ structure lies on the $\bar{3}$ axis it seemed likely at the outset of the present study that the development of the paratacamite superstructure would be related to axial Jahn–Teller distortion of the nearest-neighbour environments about the Cu atoms in the positions related to it. The Cu(2) octahedra in the $Co_2(OH)_3Cl$ structure may be stretched along Cu–Cl directions without causing a reduction of site symmetry.

Experimental

The present study was made on paratacamite from the type locality, Generosa mine, Sierra Gorda, Chile; the material was kindly donated by the British Museum from its collection (B. M. 86958). Powder and single crystal X-ray diffraction and optical examination essentially confirmed the results of Frondel (1950). However, the intensities of the reflexions characteristic of the superstructure were much weaker than expected;

with the crystal used to collect the intensity data for the crystal structure analysis, exposures of six to eight days were required to produce unambiguous reflexions on precession films. The systematic absences for both the subcell and true unit cell are hkl with $-h+k+l \neq 3n$, consistent with the space groups $R\bar{3}m$, $R3m$, $R32$, $R\bar{3}$ and $R3$. The lattice parameters of the true unit cell, determined by least-squares refinement of 12 centred reflexions measured on a four-circle diffractometer with Zr-filtered Mo $K\alpha$ ($\lambda = 0{\cdot}7107$ Å) radiation, are $a = 13{\cdot}654$ (5) Å, $c = 14{\cdot}041$ (6) Å for the hexagonal unit cell and $a = 9{\cdot}168$ (4) Å, $\alpha = 96{\cdot}263$ (3)° for the corresponding rhombohedral unit cell.

The crystal selected for the structure determination was euhedral and approximately equidimensional, with a calculated volume of $0{\cdot}32 \times 10^{-6}$ cm^3. The X-ray intensity data were collected on a Picker *FACS* 1 four-circle diffractometer system at the University of Western Ontario using a scintillation detector, Zr-filtered Mo $K\alpha$ ($\lambda = 0{\cdot}7107$ Å) radiation and the 2θ scan technique: 40 s stationary background counts, peak-base widths of $2{\cdot}5°$ 2θ (uncorrected for dispersion) and a scanning rate of $0{\cdot}5°$ per min. Data collection was terminated at $2\theta = 65°$ since the data set within that limit already included many weak reflexions and it was considered that the collection of additional data would not significantly improve the final result. The resulting data were processed by a data correction routine which corrected for background, Lorentz and polarization effects, and absorption. Transmission factors for the absorption correction were calculated by the analytical method of de Meulenaer & Tompa (1965) using a value for the linear absorption coefficient of $121{\cdot}5$ cm^{-1}. The crystal was oriented with [$\bar{1}20$] parallel to the φ axis. The calculated transmission factors varied from $0{\cdot}418$ for 214 to $0{\cdot}531$ for $20\bar{1}$. Standard deviations (σ) were calculated from the expression $\sigma = \frac{1}{2}[1/\text{Lp}T \, . \, (\sigma_p^2 + \sigma_{b1}^2 + \sigma_{b2}^2 + (0{\cdot}02I)^2)/I]^{1/2}$, where Lp is the Lorentz–polarization factor, T is the transmission factor, σ_p, σ_{b1} and σ_{b2} are, respectively, the standard deviations for the counting rates of the peak and backgrounds and I is the background-corrected peak intensity. Each reflexion whose intensity was less than the associated background plus 3σ was given zero intensity and was rejected in the structure refinements discussed in the following section. The data were collected in two stages: the intensity data for the substructure reflexions were averaged from six

equivalent sets collected in the hemisphere with k positive, whereas the intensity data for reflexions characteristic of the superstructure were averaged from the two equivalent sets hkl, $hk\bar{l}$ and $hk\bar{l}$, hkl. The final data list contained 1027 reflexions. Only 475 reflexions had non-zero intensity and of these 221 were substructure reflexions.

Crystal structure investigation

The crystal structure investigation was initiated by assuming that the substructure of paratacamite has the rhombohedral Co$_2$(OH)$_3$Cl structure type, crystallizing in space group $R\bar{3}m$ (D_{3d}^5). The substructure was refined by full-matrix, least-squares refinement using program *RFINE* (L. Finger, Geophysical Laboratory, Washington). *RFINE* minimizes the function $\sum w(|F_o| - |F_c|)^2$, where $w = 1/\sigma^2$, F_o is the observed and F_c the calculated structure factor, and calculates a conventional residual index, $\sum ||F_o| - |F_c||/\sum |F_o|$, and a weighted residual index, $[\sum w(|F_o| - |F_c|)^2/\sum wF_o^2]^{1/2}$. The scattering curves for Cu^{2+}, O$^-$ and Cl$^-$ were taken from Cromer & Mann (1968), and real and imaginary components of the anomalous dispersion coefficients for Cu and Cl were from Cromer (1965). Using the data list for the substructure reflexions, the positional parameters for Co$_2$(OH)$_3$Cl (de Wolff, 1953) with isotropic thermal parameters of $1{\cdot}0$ for all atoms resulted in a weighted residual index of $0{\cdot}20$. The structure refined within a few cycles converging on values for the weighted and conventional residual indices for anisotropic thermal parameters of $0{\cdot}022$ and $0{\cdot}019$,
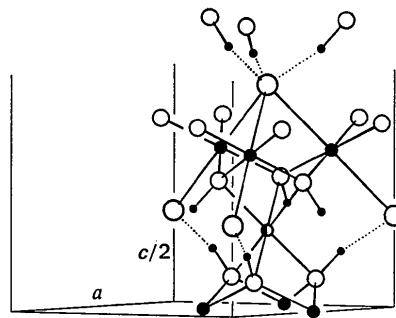

Fig. 1. Crystal structure of the paratacamite substructure – the average structure; Cu(1): medium, half-open circle; Cu(2): medium, full circles; O: medium, open circles; Cl: large, open circles; H: small, full circles.

Table 1. *Positional and anisotropic thermal parameters with their standard deviations in parentheses for the substructure of paratacamite*

Anisotropic thermal parameters ($\times 10^5$) are calculated from $T = \exp[-(\beta_{11}h^2 + \beta_{22}k^2 + \beta_{33}l^2 + 2\beta_{12}hk + 2\beta_{13}hl + 2\beta_{23}kl)]$.

	Equipoint position	x	y	z	β_{11}	β_{22}	β_{33}	β_{12}	β_{13}	β_{23}
Cu(1)	3(b)	0	0	$\frac{1}{2}$	639 (16)	639 (16)	95 (4)	319 (8)	0	0
Cu(2)	9(e)	$\frac{1}{2}$	0	0	742 (12)	624 (16)	154 (2)	312 (8)	53 (10)	26 (5)
O	18(h)	0·2064 (2)	0·7936 (2)	0·0614 (2)	1076 (73)	766 (110)	254 (12)	383 (55)	394 (47)	197 (24)
Cl	6(c)	0	0	0·1938 (1)	912 (23)	912 (23)	137 (6)	456 (12)	0	0

respectively; the standard deviation of an observation of unit weight being 0·94. The positional and thermal parameters are given in Table 1. The substructure can be considered as the average structure of paratacamite. It consists essentially of layers of Cu(2) octahedra arranged parallel to (001) and coupled together by Cu(1) octahedra (Fig. 1).

Residual peaks near the O atom positions were present on $F_o - F_c$ maps and the substructure was refined further assuming the O atoms to be disordered between two adjacent partly occupied positions. With anisotropic thermal parameters for Cu and Cl and isotropic thermal parameters for O, this refinement converged on values for the weighted and conventional residual indices of 0·021 and 0·019 respectively, the standard deviation of an observation of unit weight being 0·92. The corresponding positional and occupancy data are given in Table 2.

Table 2. *Positional and occupancy parameters for the substructure of paratacamite, refined with disordered O positions*

	Occupancy	x	y	z
Cu(1)	1	0	0	$\frac{1}{2}$
Cu(2)	1	$\frac{1}{2}$	0	0
O(1)	0·76 (9)	0·210 (1)	0·790 (1)	0·065 (1)
O(2)	0·24 (9)	0·195 (3)	0·805 (3)	0·048 (3)
Cl	1	0	0	0·1938 (1)

The determination of the full or ordered crystal structure of paratacamite was complicated by the very weak intensities of the reflexions characteristic of the superstructure. The intensity of the strongest superstructure reflexion (974) was less than 0·2% of the intensity of the strongest substructure reflexion (404) and, although 34% of the superstructure reflexions had non-zero intensity, less than 5% had non-zero intensity in both of the two equivalent data sets collected. Initial attempts with trial structures based on ordered arrangements of the O atoms were unsuccessful. The true structure emerged by refinement of the Cu and Cl positions of a trial structure in space group

$R\overline{3}$ in which the O positions had been estimated from $F_o - F_c$ maps. The refinement of the full structure converged on values for the weighted and conventional residual indices of 0·036 and 0·051 respectively, the standard deviation for an observation of unit weight being 1·19. The positional and thermal parameters are given in Table 3. Anisotropic thermal parameters were used for three of the Cu positions. Refinement with all isotropic thermal parameters converged on values for the weighted residual indices of 0·043 and 0·060 respectively, the standard deviation for an observation of unit weight being 1·39. The weighted residual index for the former refinement is significant at the 0·005 level, the dimension of the hypothesis being 15 (Hamilton, 1965). The observed and calculated structure factors for the refinement with anisotropic thermal parameters are given in Table 4* and do not include data for the reflexions of zero intensity. In regard to the data for the superstructure reflexions the agreement between F_o and F_c is much better for those reflexions which have non-zero intensity in both of the equivalent data sets collected. Clearly, most of the superstructure reflexions recorded as having non-zero intensity were at or near the limit of detectability of the recording method used.

Hydrogen atoms

A residual peak at $x = 0·14$, $y = 0·28$, $z = 0·12$ in the $F_o - F_c$ map for the average substructure structure was attributed to the H atom position. The peak height was 1·2 e Å^{-3}, somewhat greater than expected. An attempt was made to minimize this peak interference by computing the difference synthesis with lower $\lambda^{-1} \sin \theta$ cut-off values (La Placa & Ibers, 1965), but with a $\lambda^{-1} \sin \theta$ limit of 0·35 Å^{-1} there were too few terms remaining and the difference maps were fairly feature-

---

* Tables 4, 5 and 6 have been deposited with the British Library Lending Division as Supplementary Publication No. SUP 30642 (5pp.). Copies may be obtained from The Executive Secretary, International Union of Crystallography, 13 White Friars, Chester CH1 1NZ, England.

Table 3. *Positional and thermal parameters with their standard deviations in parentheses for the ordered structure of paratacamite*

Anisotropic thermal parameters ($\times 10^5$) calculated as in Table 1.

	Equivalent subcell site	Equipoint position	x	y	z	$\beta_{11}(B)$	β_{22}	β_{33}	β_{12}	β_{13}	β_{23}
Cu(1)	Cu(1)	3(b)	0	0	$\frac{1}{2}$	0·69 (7)					
Cu(2)	Cu(1)	9(d)	$\frac{1}{2}$	$\frac{1}{2}$	$\frac{1}{2}$	159 (20)	184 (20)	102 (7)	87 (19)	1 (15)	−17 (16)
Cu(3)	Cu(2)	18(f)	0·4133 (3)	0·3302 (2)	0·3318 (2)	179 (13)	156 (12)	200 (11)	94 (11)	−11 (10)	19 (10)
Cu(4)	Cu(2)	18(f)	0·4119 (2)	0·5778 (2)	0·3326 (2)	145 (13)	134 (11)	107 (9)	64 (11)	−19 (9)	−11 (9)
O(1)	O	18(f)	0·5593 (10)	0·6180 (9)	0·4047 (8)	0·58 (15)					
O(2)	O	18(f)	0·5640 (10)	0·4322 (10)	0·3908 (11)	0·77 (17)					
O(3)	O	18(f)	0·3666 (15)	0·4284 (14)	0·3905 (13)	2·51 (29)					
O(4)	O	18(f)	0·0643 (10)	0·1255 (11)	0·3921 (12)	1·06 (20)					
Cl(1)	Cl	6(c)	0	0	0·1954 (6)	1·19 (10)					
Cl(2)	Cl	18(f)	0·5004 (4)	0·5026 (5)	0·1933 (2)	1·18 (4)					

less. Residual peaks were also present in corresponding areas of the difference map for the ordered paratacamite structure. They were weaker and more diffuse than that for the average structure and did not allow precise location of the four non-equivalent positions. However their peak heights were relatively enhanced when the maps were computed at lower $\lambda^{-1} \sin \theta$ cut-off values, 0·45 and 0·35 Å^{-1}, and this tends to confirm the general location of the H atom position in the average structure (Fig. 1).

The H atoms form O–H$\cdots$Cl associations as expected. In the average structure the relevant interatomic distances are O–H = 1·14 Å, H–Cl = 1·95 Å, O–Cl = 3·07 Å, and the O–H–Cl bond angle is 165·7°. These data are reasonably consistent with those for CuCl₂.2H₂O (Peterson & Levy, 1957) and methylglyoxal bisguanylhydrazone dihydrochloride monohydrate (Hamilton & La Placa, 1968) in which the H atoms were located more precisely, through neutron diffraction data.

Discussion

The present investigation has shown that paratacamite crystallizes in space group $R\bar{3}$, with $Z = 24$. The Cu atoms are accommodated in four non-equivalent positions. Selected interatomic distances and bond angles are given in Tables 5 and 6,* respectively: Cu–(O,Cl) distances are summarized in Fig. 2 and are compared with data for atacamite and botallackite in Table 7. The Cu(3) and Cu(4) positions are derived from the Cu(2) position of the average structure. The nearest-neighbour environments about these two positions are quite similar and the means of the distances to the four

* See footnote on p. 185.

nearest O atoms and to the two distant Cl atoms are comparable to the data for the Cu(1) polyhedron in atacamite. The nearest-neighbour environments of the Cu(1) and Cu(2) positions, which are derived from the Cu(1) position of the average structure, are unusual for Cu²⁺ atoms. Cu(2) has two near and four distant O atom neighbours and the Cu(1) position, lying on

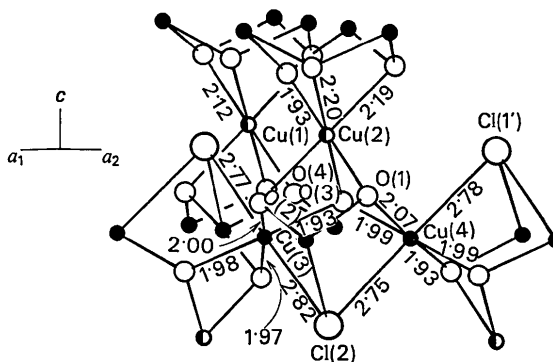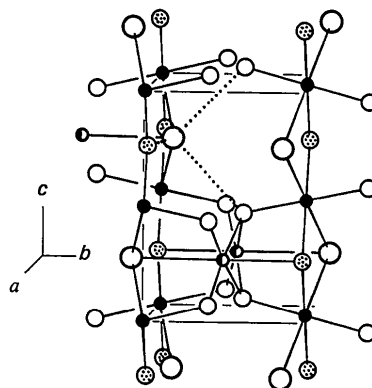Fig. 2. Part of the crystal structure of paratacamite; bond distances in Å.

Fig. 3. Hydrogen-bonding scheme for atacamite; Cu(1): small, full circles; Cu(2): small, half-open small circles; O(1): medium, stippled circles; O(2): medium, open circles; Cl: large, open circles.
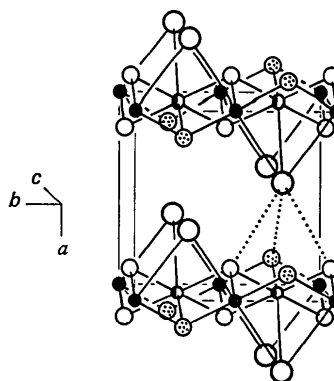
Table 7. *Nearest-neighbour Cu octahedra in* Cu₂(OH)₃Cl *phases*

Phase	Position	Proportion of Cu	Number and distances (Å) of Cu neighbours	
			Near	Distant
Atacamite	Cu(1)	½	2, –O = 2·00	2, –Cl = 2·76
(Wells, 1949)			2, –O = 2·04	
	Cu(2)	½	2, –O = 1·94	1, –Cl = 2·76
			2, –O = 2·07	1, –O = 2·36
Botallackite	Cu(1)	½	2, –O = 1·86	2, –Cl = 2·91
(Voronova &			2, –O = 1·95	
Vainshtein, 1958)				
	Cu(2)	½	4, –O = 1·97	1, –Cl = 2·86
				1, –O = 2·37
Paratacamite	Cu(3)	³⁄₈	1, –O = 1·93	1, –Cl = 2·770
			1, –O = 1·97	1, –Cl = 2·818
			1, –O = 1·98	
			1, –O = 2·00	
	Cu(4)	³⁄₈	1, –O = 1·93	1, –Cl = 2·753
			2, –O = 1·99	1, –Cl = 2·778
			1, –O = 2·07	
	Cu(2)	³⁄₁₆	2, –O = 1·93	2, –O = 2·19
				2, –O = 2·20
	Cu(1)	¹⁄₁₆	6, –O = 2·12	

Fig. 4. Hydrogen-bonding scheme for botallackite; symbols as for Fig. 3.

the $\bar{3}$ axis, has six equivalent O atom neighbours at intermediate Cu–O bond distances (2·12 Å).

The structure of paratacamite illustrates very well that the development of polyhedral distortions in response to the Jahn–Teller effect can be inhibited by constraints imposed by the crystal structure. Dunitz & Orgel (1960) have pointed out that, whilst the short bond distances to common anions (or ligands) in Cu^{2+} coordination polyhedra show little variation, the stretched distances may show a wide variation. Stretched Cu–Cl distances vary from 2·65 to 3·05 Å; the shorter distances are found in 'three-dimensional' structures (for example, atacamite, Fig. 3) and the longer distances in layer structures (for example, botallackite, Fig. 4). In paratacamite, the Cu(1) and Cu(2) polyhedra couple the layers of Cu(3) and Cu(4) polyhedra, and bonds to Cu(3) and Cu(4) atoms constrain the nearest-neighbour O atoms of the Cu(1) and Cu(2) positions and prevent the development of (4 + 2) configurations. The (2 + 4) configuration occurs in K_2CuF_4 (Knox, 1959) and in several M^+CuF_3 compounds (Cotton & Wilkinson, 1966, p. 899). However, a Cu^{2+} polyhedral configuration similar to that of Cu(1), with six equivalent Cu–anion bond lengths, has not been reported previously.

Each Cu polyhedron shares six polyhedral edges with adjacent polyhedra (Fig. 2). The O–Cu–O and O–Cu–Cl bond angles associated with these shared edges are all markedly less than 90° (ranging from 74·6 to 85·5°) and these are the principal angular distortions in the Cu polyhedra. The acute bond angles clearly result from stretching of the Cu–Cu distances associated with the shared edges and this is attributable to electrostatic repulsion between the positively charged metal atoms (Pauling, 1960, p. 559). Now, the lobes of the t_{2g} set of $3d$ orbitals on transition metals must project toward octahedral coordination edges. However, in paratacamite it appears that the electrons in these orbitals do not neutralize the effective positive charges on the Cu^{2+} atoms along Cu–Cu directions.

The hydrogen bonds to the Cl atoms must supplement the Cu(1)–O and Cu(2)–O bonds in coupling the layers of Cu(3) and Cu(4) polyhedra. The O atoms in paratacamite are coordinated tetrahedrally to three Cu and one H. However, the Cu–O–Cu bond angles generally depart considerably from the ideal tetrahedral bond angle (ranging from 92·7° to 122·0°). The two non-equivalent Cl positions are each coordinated in a 'trigonal prismatic' arrangement to three Cu atoms and three H atoms. The Cl atoms are only feebly bonded in the structure since the Cu–Cl σ bonds are weakened by the filled $\sigma^*(e_g)$ antibonding orbitals and the associations with the H atoms are *via* hydrogen bonds.

Earlier investigations have not located the H atom positions in the crystal strucures of either bottallackite or atacamite. By analogy with paratacamite, the H atoms in botallackite are probably associated with the O,Cl pairs indicated in Fig. 4, for which O(1)–Cl = 3·30 Å and O(2)–Cl = 3·10 Å. The resulting hydrogen bonds to the Cl atoms would be the primary bonding forces coupling the layers of Cu(1) and Cu(2) polyhedra in the botallackite structure. Similarly, in atacamite, H···Cl bonds across the honeycomb voids help to couple the layers of Cu(1) and Cu((2) polyhedra; the related O–Cl distances being O(1)–Cl = 2·84 Å, O(2)–Cl = 3·07 Å. In botallackite and atacamite the O(1)–Cl distances associated with H atom positions are, respectively, longer and shorter than expected and this may be attributed to displacement of the O(1) atoms due to stretching of the Cu(2)–O(1) bond distances.

References

BRASSEUR, H. & TOUSSAINT, J. (1942). *Bull. Roy. Soc. Sci. Liège*, **11**, 555–566.
COTTON, F. A. & WILKINSON, G. (1966). *Advanced Inorganic Chemistry*, 2nd ed. New York: Interscience.
CROMER, D. T. (1965). *Acta Cryst.* **18**, 17–23.
CROMER, D. T. & MANN, J. B. (1968). *Acta Cryst.* A **24**, 321–323.
DUNITZ, J. D. & ORGEL, L. E. (1960). *Advanc. Inorg. Chem. Radiochem.* **2**, 1–60.
FRONDEL, C. (1950). *Miner. Mag.* **29**, 34–45.
HAMILTON, W. C. (1965). *Acta Cryst.* **18**, 502–510.
HAMILTON, W. C. & LA PLACA, S. J. (1968). *Acta Cryst.* B **24**, 1147–1156.
KNOX, K. (1959). *J. Chem. Phys.* **30**, 991–993.
LA PLACA, S. J. & IBERS, J. A. (1965). *Acta Cryst.* **18**, 511–519.
MEULENAER, J. DE & TOMPA, H. (1965). *Acta Cryst.* **19**, 1014–1018.
OSWALD, H. R. & FEITKNECHT, W. (1964). *Helv. Chim. Acta*, **47**, 272–289.
PAULING, L. (1960). *The Nature of the Chemical Bond*, 3rd ed. Ithaca: Cornell Univ. Press.
PETERSON, S. W. & LEVY, H. A. (1957). *J. Chem. Phys.* **26**, 220–221.
SHARKEY, J. B. & LEWIN, S. Z. (1971). *Amer. Min.* **56**, 179–192.
SMITH, G. F. H. (1906). *Miner. Mag.* **14**, 170–177.
VORONOVA, A. A. & VAINSHTEIN, B. K. (1958). *Sov. Phys. Crystallogr.* **3**, 445–451.
WELLS, A. F. (1949). *Acta Cryst.* **2**, 175–180.
WOLFF, P. M. DE (1953). *Acta Cryst.* **6**, 359–360.